Journal of Industrial and Engineering Chemistry 17 (2011) 352–357

Contents lists available at ScienceDirect

Journal of Industrial and Engineering Chemistry

journal homepage: www.elsevier.com/locate/jiec

Synthesis and electroluminescence properties of fluorene–anthracene based copolymers for blue and white emitting diodes

Ho Jun Song, Jang Yong Lee, In Sung Song, Doo Kyung Moon, Jung Rim Haw *

Department of Material Chemistry and Engineering, Konkuk University, Gwangjin-gu, 1 Hwayang-dong, Seoul 143-701, Republic of Korea

ARTICLE INFO

Article history:
Received 26 July 2010
Accepted 9 September 2010
Available online 2 March 2011

Keywords:
Fluorene
Anthracene
Conjugated polymer
PLED
Electroplex

ABSTRACT

We have synthesized poly(9,9-dioctylfluorene-co-9,10-diphienylanthracene) (PFAN), which is based on the blue light-emitting materials fluorene and anthracene derivative, using Suzuki coupling. These copolymers synthesized at wide-ranging mol ratios are fully dissolved in ordinary organic solvents and show high thermal stability. PF50AN50, PF75AN25, and PF90AN10 demonstrate maximum photoluminescent wavelengths when λ_{max} = 440, 440, and 443 nm and peaks for electroluminescent properties when λ_{max} = 442, 442, and 450 nm, respectively. In all PFAN series, new electroplex-increased emission peaks appear nearby 540 nm at 13 V, 14 V, and 15 V, respectively, as driving voltage increases, with the CIE coordinates being (0.30, 0.36) and change in color observed from blue emission to white emission.

1. Introduction

For the past several decades, π-conjugated polymer has drawn keen academic attention in a wide variety of fields including organic light-emitting diodes (OLEDs) [1–5], organic thin film transistors (OTFTs) [6–11], organic photovoltaic cells (OPVs) [12–15], and optical devices [16,17], with OLEDs currently being one of the most attractive applications. Unlike conventional devices of liquid crystal display (LCDs) and cathode ray tubes (CRTs), an OLED is a self-emitting device that does not require any backlight and has a wide-viewing angle. It also enables the production of ultra-lightweight thin films and offers many outstanding properties such as low operating voltage and fast response time. Polymer light-emitting diodes (PLEDs), in particular, are widely expected to be the next major advance in the display industry, as they can cover large areas based on screen printing in the production process—compared to a small-molecule OLED utilizing a high vacuum deposition technique—and are flexible enough to realize the production of flexible displays [18–20].Since the discovery of poly(phenylenevinylene) in 1990, numerous studies have been undertaken to realize a wide array of colors [21]. Created as part of such endeavors are: blue light-emitting materials such as polyfluorene [22], poly(fluorene-phenothiazine) [23], and poly-carbazole [24]; poly(phenylene-vinylene) conductor [25] and other green light-emitting materials; and orange and red light-emitting materials such as poly(fluorene-thiophene) [7], poly(-fluorene-benzothiophene) [26], and poly(fluorene-phenothiazine) conductor [27]. These materials displaying red, green, and blue (RGB) can be used to successfully realize full-color displays. At present, however, green and orange devices are the only two options that are commercially viable, while blue and red light-emitting diodes are still in their infancy [28,29].The blue light-emitting material poly(9,9-di-n-hexylfluorene) (PDHF) was the first to be developed among these devices, and active research has since been underway on various types of polyfluorene derivatives, given fluorene's high photoluminescence quantum yield, excellent chemical/thermal stability, good solubility and uniform film generation, high molecular content, and ease of synthesis [30–32]. Polyfluorene is also widely used in many studies on white light-emitting materials owing to the aforementioned advantages [33–35]. Rigid-rod polyfluorene, however, generally shows a nematic-type arrangement due to π–π stacking-induced chain aggregation upon the generation of a film. This chain aggregation reduces luminescence quantum yield, and hence some researchers are applying the bulky aryl group or alkyl chain to the ninth position of fluorene to minimize chain aggregation and achieve high light-emitting efficiency [36,37].

Numerous studies are also being carried out regarding anthracene conductor as another blue light-emitting material, as it has excellent physical properties, high power/current efficiency, and outstanding external quantum yield. Especially noteworthy is that anthracene, which has bulky substituents in the ninth and tenth

* Corresponding author. Tel.: +82 2 450 3499.
E-mail address: jrhaw@konkuk.ac.kr (J.R. Haw).

1226-086X/$ – see front matter © 2011 The Korean Society of Industrial and Engineering Chemistry. Published by Elsevier B.V. All rights reserved.
doi:10.1016/j.jiec.2011.02.038

positions, was twisted by mutual interactions between these bulky substituents and demonstrated a non-planar structure. Such non-planarity of the structure effectively reduced intermolecular π–π stacking and minimized concentration quenching. Consequently, the non-planarity of anthracene conductor facilitates generation of a stable amorphous film and effective EL properties [38,39].

Against this background, we used a fluorene conductor with high PL/EL quantum efficiency and a non-planar phenylanthracene conductor to synthesize—using the Suzuki coupling method—polyfluorene and three new types of poly(9,9-dioctylfluorene-co-9,10-diphenylanthracene). Effective blue light emission, at anthracene derivative mol ratios of 50%, 25%, and 10%, respectively, was obtained. The chemical structure and the synthetic procedure of the new polymer, PFAN series, are shown in Scheme 1. Anthracene derivative mol ratio of PF50AN50, PF75AN25, PF90AN10 are respectively 50%, 25%, 10%.

2. Experiment

Unless otherwise specified, all the reactions were carried out under nitrogen atmosphere. Solvents were dried by standard procedures. All column chromatography was performed with the use of silica gel (230–400 mesh, Merck) as the stationary phase. ^{1}H NMR spectra were performed in a Bruker ARX 400 spectrometer using solutions in $CDCl_3$ and chemical were recorded in ppm units with TMS as the internal standard. Electronic absorption spectra were measured in chloroform using a HP Agilent 8453 UV–vis spectrophotometer. Photoluminescent spectrum was recorded by Perkin Elmer LS 55 luminescence spectrometer. Cyclic voltammetry experiments were performed with a Zahner IM6eX Potentionstat/Galvanostat. All measurements were carried out at room temperature with a conventional three-electrode configuration consisting of platinum working and auxiliary electrodes and a non-aqueous Ag/AgCl reference electrode at the scan rate of 50 mV/s. The solvent in all experiments was acetonitrile and the supporting electrolyte was 0.1 M tetrabutyl ammonium-hexafluorophosphate. DSC measurements were carried out using a TA instruments DSC 2310 Modulated DSC at a heating rate of 10 °C/min. TGA measurements were performed on NETZSCH TG 209 F3 thermogravimetric analyzer. All GPC analyses were made using THF as eluant and polystyrene standard as reference. Fabricated device

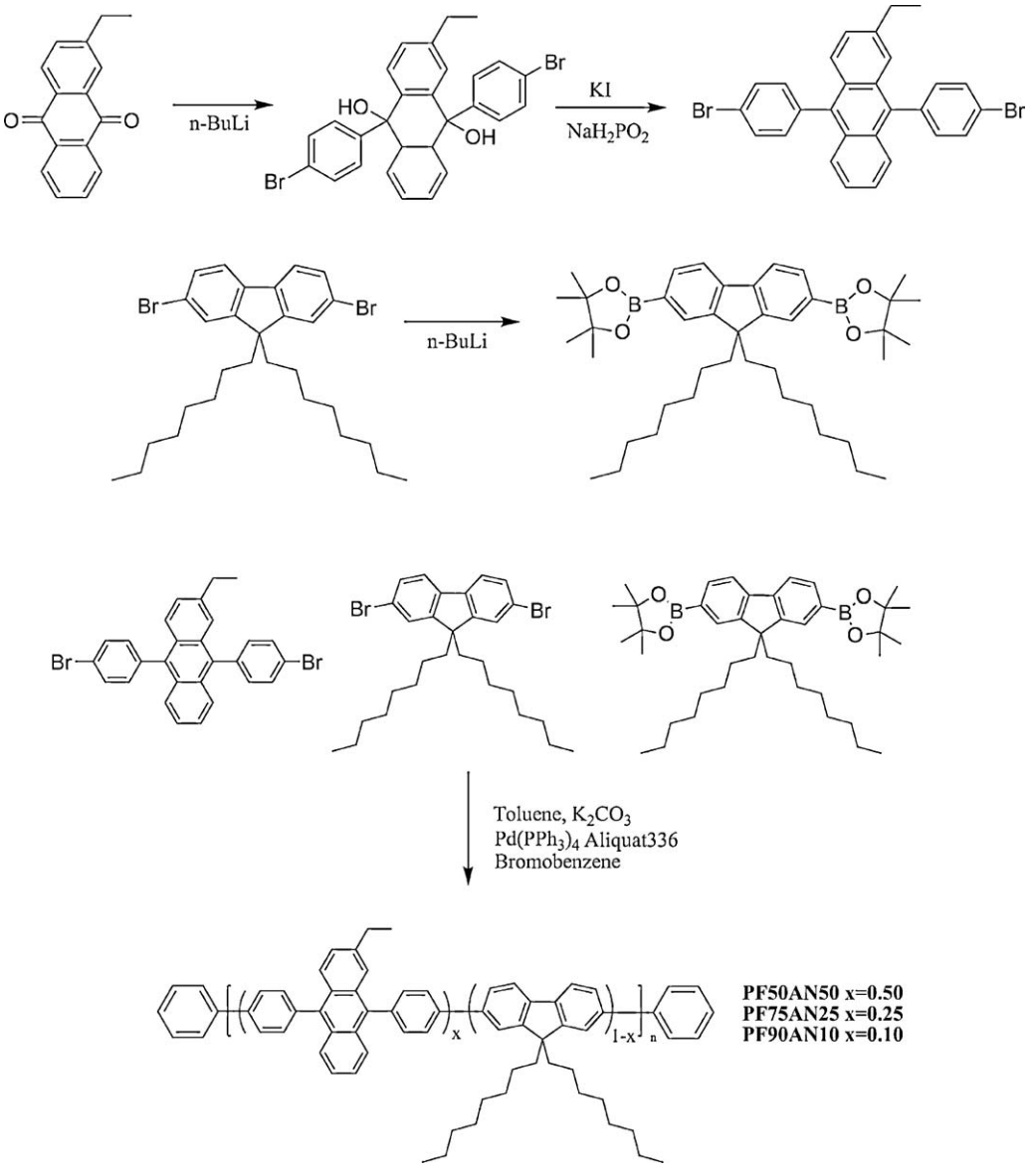

Scheme 1. Synthetic scheme of the polymers.

structure were ITO/PEDOT:PSS/polymer/BaF_2/Ba/Al. PEDOT:PSS and polymer film were fabricated by spin-coating method.

2.1. Preparation of 9,10-bis(4-bromophenyl)-2-ethylanthracene

To 1,4-dibromobenzene (10.48 g, 44.43 mmol) dissolved in THF (30 mL) was added 27.76 mL of *n*-butyllithium (1.6 M in hexane) slowly at −78 °C. To the suspension, 2-ehtylanthraquinone (5 g, 21.16 mmol) in THF (30 mL) was added dropwise at −78 °C. The mixture was left to reach room temperature. Cold water (200 mL) was added and the organic phase separated. The water phase was extracted with ether (300 mL). The combined organic fractions were dried over sodium sulfate and the solvent was removed at a reduced pressure. To this residue were added potassium iodide (10.45 g, 63 mmol), sodium hypophosphite hydrate (18.47 g, 210 mmol), and acetic acid (50 mL), and the mixture was heated under reflux for 4 h. After cooling, the product washed with plenty of water, and dried. The compound was purified by column chromatography over silica gel. Yield 9.60 g (88%). ^{1}H NMR (400 MHz, $CDCl_3$, δ, ppm): 1–3 (5H, CH_2, CH_3), 7–8 (15H, ArH).

2.2. Preparation of 2,2′-(9,9-dioctyl-9H-fluorene-2,7-diyl)bis(4,4,5,5-tetramethyl-1,3,2-dioxaborolane)

To 9,9-dioctyl-2,7-dibromofluorene (1.5 g, 2.73 mmol) dissolved in THF (20 mL) was added 3.58 mL of *n*-butyllithium (1.6 M in hexane) slowly at −78 °C. To the suspension, 2-Isopropoxy-4,4,5,5-tetramethyl-1,3,2-dioxaborolane (1.22 mL, 6 mmol) was added dropwise at −78 °C. The mixture was left to reach room temperature. Cold water (200 mL) was added and the organic phase separated. The water phase was extracted with ether (300 mL). The combined organic fractions were dried over sodium sulfate and the solvent was removed at a reduced pressure. The product was purified by recrystallization in hexane. Yield 1.03 g (60%) ^{1}H NMR (400 MHz, $CDCl_3$, δ, ppm): 1–3 (46H, CH_2, CH_3), 7–8 (6H, ArH).

2.3. Polymerization of poly(9,9-dioctylfluorene-co-9,10-diphenylanthracene)

9,10-Bis(4-bromophenyl)-2-ethylanthracene and 2,2′-(9,9-dioctyl-9H-fluorene-2,7-diyl)bis(4,4,5,5-tetramethyl-1,3,2-dioxaborolane), 9,9-dioctyl-2,7-dibromofluorene, $(PPh_3)_4Pd(0)$ (1.5 mol%) and Aliquat 336 were dissolved in a mixture of toluene and an aqueous solution of 2 M K_2CO_3. The solution was refluxed for 48 h with vigorous stirring in a nitrogen atmosphere. The whole mixture was poured into methanol. The precipitate was filtered off, purified with acetone, chloroform in soxlet.

PF50AN50: Yield: 0.70 g (70%). ^{1}H NMR (400 MHz, $CDCl_3$, δ, ppm): 1–3 (47H, CH_2, CH_3), 7–8 (21H, ArH).

PF75AN25: Yield: 0.63 g (63%). ^{1}H NMR (400 MHz, $CDCl_3$, δ, ppm): 1–3 (47H, CH_2, CH_3), 7–8 (13H, ArH).

PF90AN10: Yield: 0.54 g (54%). ^{1}H NMR (400 MHz, $CDCl_3$, δ, ppm): 1–3 (47H, CH_2, CH_3), 7–8 (6.6H, ArH).

3. Results and discussion

We synthesized all polymers based on Suzuki coupling using monomer 9,10-bis(4-bromophenyl)-2-ethylanthracene, 2,2′-(9,9-dioctyl-9H-fluorene-2,7-diyl)bis(4,4,5,5-tetramethyl-1,3,2-dioxaborolane) and 9,9-dioctyl-2,7-dibromofluorene. The synthesized polymers were refined with methanol, acetone, hexane, and chloroform sequentially using soxlet. They were easily dissolved in ordinary organic solvents, including chloroform, toluene, xylene, and benzene, and most generated films without difficulty. As described in Fig. 1, ^{1}H NMR showed that the polymers were successfully synthesized. The spectrum of the aromatic ring for the PFAN series was observed at 7.2–8.0 ppm, and that of the alkyl side chain was found at 0.8–2.8 ppm. The aromatic content of the anthracene core was smaller when the ratio of anthracene conductor was lower. Each polymer was measured using GPC, and the results are presented in Table 1. The Mn content in PF50AN50, PF75AN25, and PF90AN10 was relatively high, at 17,935, 22,100, and 17,001, respectively; their PDI content stood at 1.92, 1.71, and 1.37, respectively.

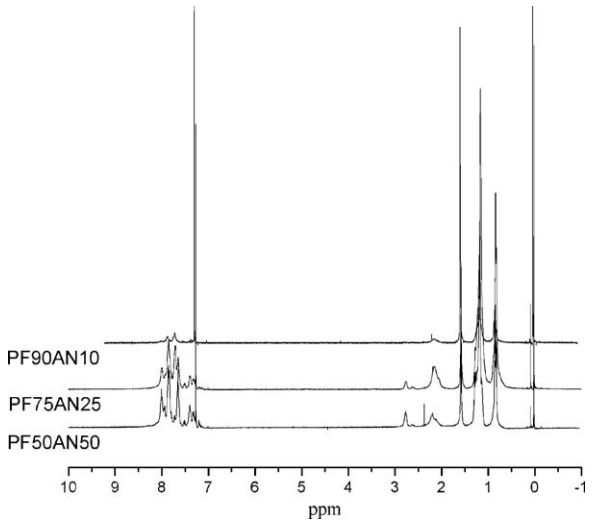

Fig. 1. ^{1}H NMR spectrum of PFAN series.

The thermal properties of the polymers were verified using TGA and DSC. Fig. 2 illustrates the TGA of the polymers. The thermal stability of the PFAN series was high enough to show 5% weight loss at 405 °C, 405 °C, and 407 °C, respectively. The polymers were scanned at a rate of 10 °C/min and underwent DSC measurement, and the *Tg* of the polymers stood at 142–147 °C. On the basis of this high thermal stability, these polymers are expected to prove stable in the manufacturing or operation of devices at high temperature.

Table 1
Physical and thermal properties of the polymers.

Polymer	M_n	M_w	PDI	T_d (°C)
PF50AN50	17,933	34,526	1.92	405
PF75AN25	22,100	37,904	1.71	405
PF90AN10	17,001	23,443	1.37	407
PF	14,181	25,586	1.80	410

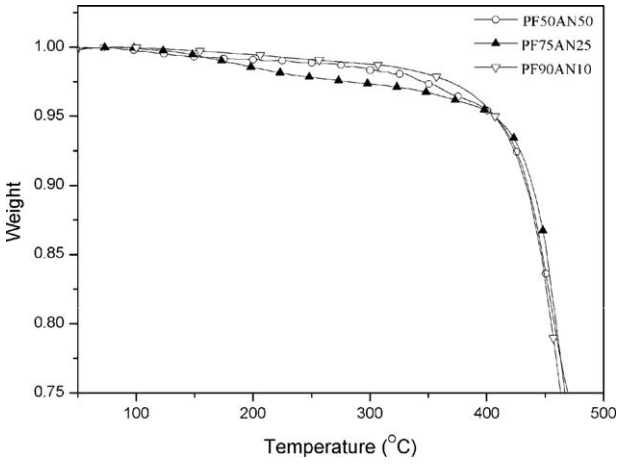

Fig. 2. TGA curve of PFAN series.

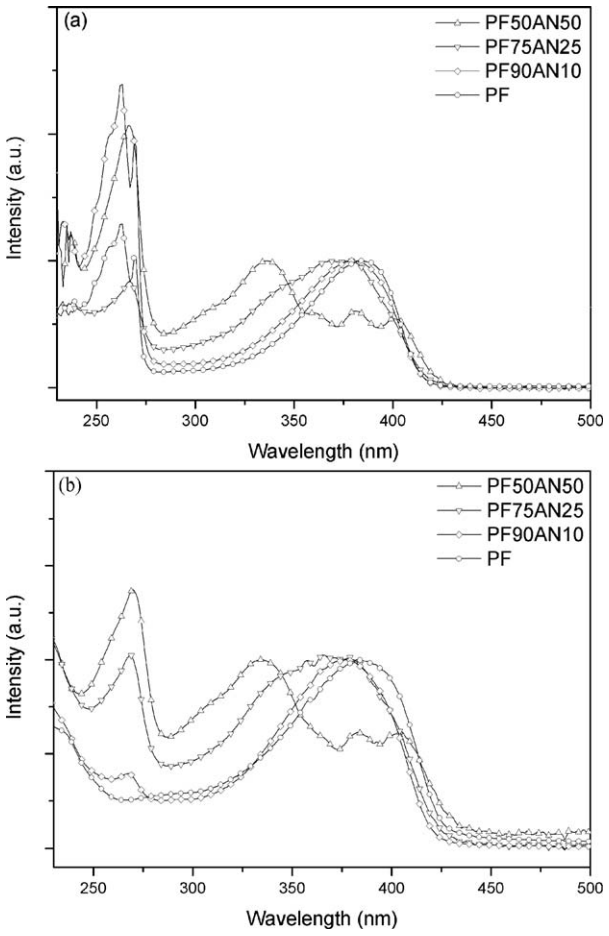

Fig. 3. UV–vis spectroscopy (a) solution (b) film of polymers.

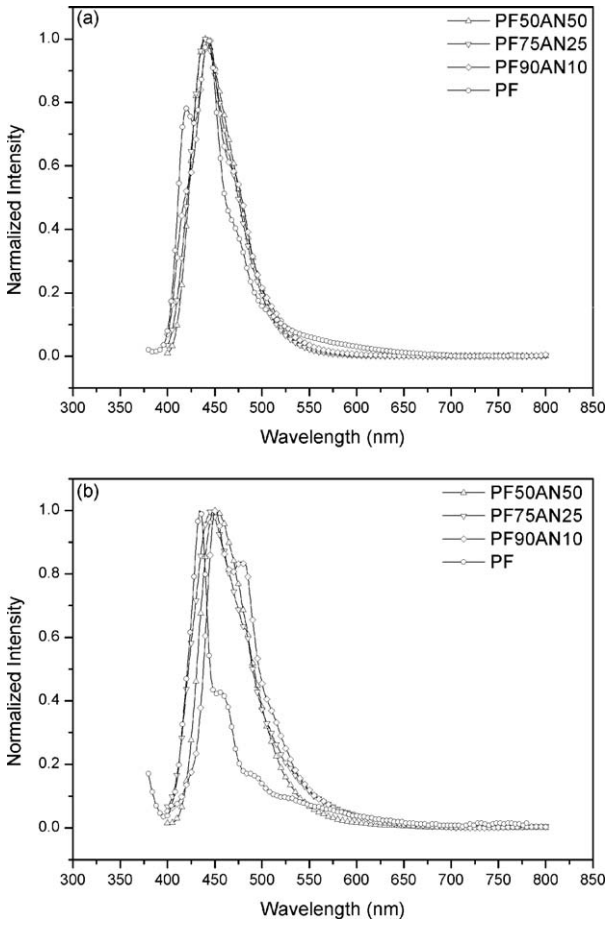

Fig. 4. PL spectroscopy (a) solution (b) film of polymers.

The polymer films were dissolved in chloroform so that the UV–vis absorption spectrum and PL spectrum could be measured from both solution and film forms. The results are illustrated in Figs. 3 and 4. The UV spectrum of PF50AN50 was similar to that of the anthracene group (λ_{max} = 340, 360, 378, 396). This is believed to be because conjugation between the anthracene core and the aromatic group in the polymer conductor was not sufficiently active [40]. The similarity to PF's UV spectrum increased as the content of anthracene core declined further. The band gap energy between the highest occupied molecular orbital (HOMO) and the lowest unoccupied molecular orbital (LUMO) was found using the UV spectrum's onset value, with PF50AN50, PF75AN25, and PF90AN10 demonstrating values of 2.93, 2.97, and 2.99 eV. PF50AN50, PF75AN25, and PF90AN10 showed respective maximum light-emitting peaks at 440 nm, 440 nm, and 443 nm in solution form and at 448 nm, 447 nm and 451 nm in the form of film, red-shifting by approximately 7–8 nm compared to the solution. This is presumably due to the impact of intermolecular interactions caused by π–π stacking. The same shoulder peak as that found in PF's PL spectrum was observed as the content of fluorene conductor was increased. The optical properties of the PFAN series are summarized in Table 2.

We used the onset value of cyclic voltammetry to derive HOMO and LUMO levels, and the results are shown in Fig. 5. The scan rate of cyclic voltammetry was set at 50 mV/s, and Ag/AgCl was used as reference electrode. The value was calibrated, with ferrocene as the standard, and substituted into the following equation to derive the HOMO level.

$$\text{HOMO level(ev)} = -4.8 - (E_{onset} - E_{1/2}(\text{ferrocene})) \quad (1)$$

Using this equation, we found that the HOMO levels of PF50AN50, PF75AN25, PF90AN10, and PF stood at 6.01, 5.97, 5.85, and 5.79 eV, respectively; we also derived their LUMO levels using the band gap energy obtained from the UV absorption. The low band gap properties became more apparent and the HOMO level declined as the content of anthracene conductor increased. Table 3 summarizes the electrochemical properties of the PFAN series.

The electroluminescent properties of the PFAN series are described in Fig. 6. Single layer emitting diodes (LED) were manufactured with ITO/PEDOT:PSS/polymer/BaF_2/Ba/Al as the structure. The maximum EL emission peak of PF50AN50, PF75AN25, and PF90AN10 ranged from 442 nm to 450 nm—similar to the PL emission peak in the form of film, or blue-shifted by around 6 nm. The turn-on voltage of the manufactured PF50AN50, PF75AN25, and PF90AN10 devices was low, at 5 V. PF75AN25 demonstrated the highest levels of brightness and efficiency, as the molecular content was relatively higher [41]. As illustrated in Table 4, PF50AN50, PF75AN25, and PF90AN10 showed maximum luminance levels of 145, 285, and 154 cd/m^2

Table 2
Optical properties of polymer.

Polymers	λ_{max} (nm)		λ_{max} (nm)		E_{opt} (eV)
	UV solution	UV film	PL solution	PL film	
PF50AN50	336, 381, 399	334, 383, 404	440	448	2.93
PF75AN25	378	379	440	447	2.97
PF90AN10	380	377	443	451, 477	2.99
PF	384	382	442	434, 450	3.00

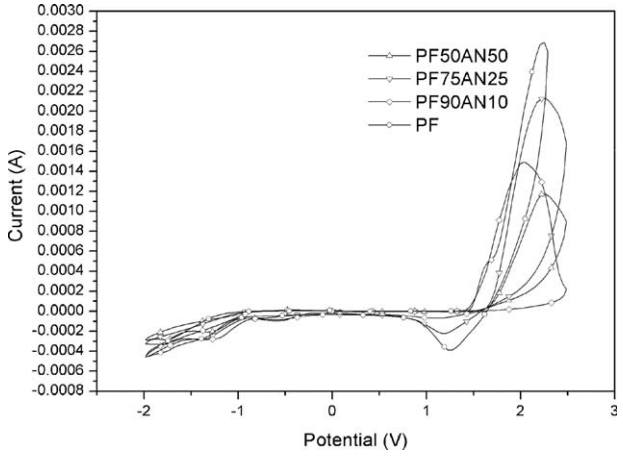

Fig. 5. Cyclic voltammogram of PFAN series.

respectively; their CIE coordinates were (0.20, 0.22), (0.23, 0.28), and (0.20, 0.23), indicating bright blue emission. It should be noted that, as Fig. 6 suggests, all of the PFAN series showed broader green and red areas and emitted white light as the voltage was increased. For instance, PF50AN50, PF75AN25, and PF90AN10 were displayed as broad areas with their shoulder emission peaks (544, 538, and 538 nm) appearing at 13 V, 14 V, and 15 V, respectively; the CIE coordinates were (0.30, 0.36), and white light emitting 20–30 cd/m^2 was observed. This, we believe, was affected by electroplex between intermolecular and intramolecular interactions, but electroplex is seen only in high driving voltage areas, not in the case of photoluminescence [42–44]. According to the Kalinowski model, when electron excitation takes place within D^+ and A^-, the following two configurations are created: (a) a local excited configuration $|A^*D)$; and (b) a charge transfer configuration $|A^-D^+)$. These two configurations can be expressed as the following equation.

$$\Psi_{EX} = C_1 \cdot |A^*D) + C_2|A^-D^+ \quad (2)$$

C_1 and C_2 represent two types of constants on expressed mixability; A*D) refers to the electron transition from A to D (i.e. recombination of the energy level electron in A and HOMO energy level hole in D) [45–48]. Fig. 7 shows a band diagram illustrating an electroplex caused by polymer intramolecular and intermolecular interactions. As the voltage rose, electrons increased from the (a) recombination form to the (b) recombination form, showing long-pulse energy and resulting in a color shift. Considering that new emission peaks appeared in PF50AN50, PF75AN25, and PF90AN10 at 13 V, 14 V, and 15 V, respectively, we concluded that electroplex-increased electron transitions increased between fluorene conductors as anthracene conductors grew in number. This demonstrates that electroplex, a phenomenon observed primarily in blending and interfaces, may also take place in a single component due to the influence of intramolecular and intermolecular interactions.

Table 3
Electrochemical properties of the polymers.

Polymer	Oxidation onset	HOMO (eV)	LUMO (eV)	Optical band gap (eV)
PF50AN50	1.67	−6.01	−3.08	2.93
PF75AN25	1.63	−5.91	−3.00	2.97
PF90AN10	1 51	−5.85	−2.86	2.99
PF	1.45	−5.79	−2.79	3.00

HOMO = $-4.8(E_{onset} - E_{1/2}$(ferrocene)).
LUMO = E_{opt} − HOMO.

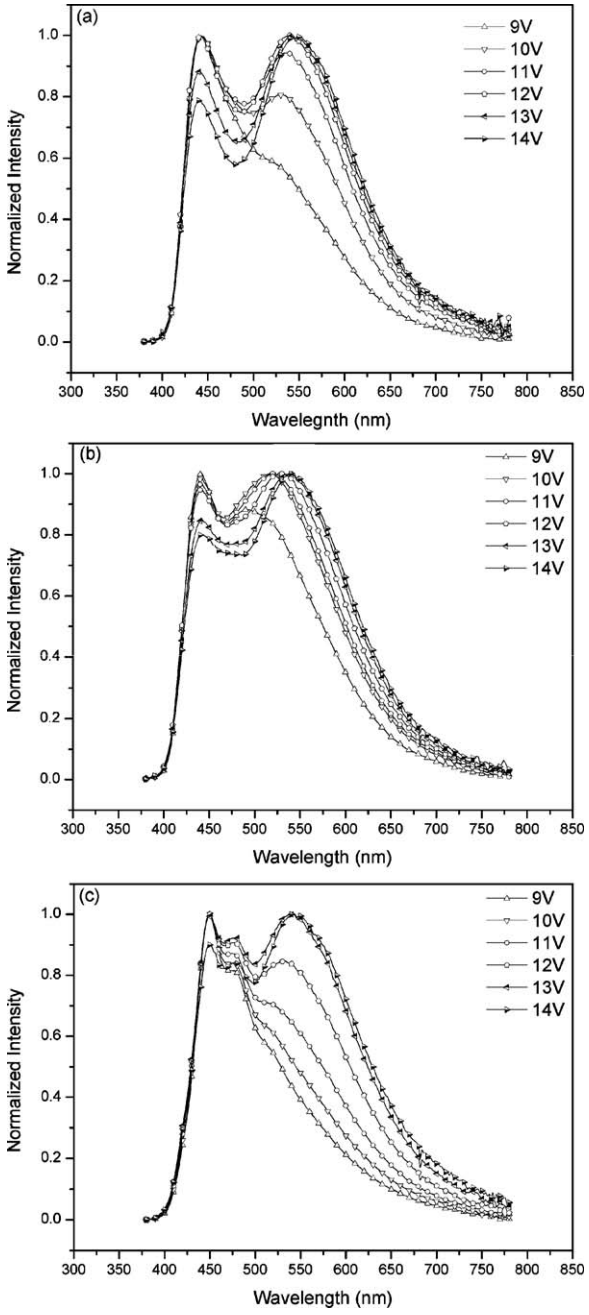

Fig. 6. EL luminescent spectra of (a) PF50AN50 (b) PF75AN25 (c) PF90AN10 with driving voltage.

We plan to design a new copolymer using blue green materials with different band gap energies to gauge the possibility of realizing electroplex phenomena. The EL properties of the PFAN series are summarized in Table 4.

Table 4
EL properties of polymers.

Polymers	EL emission λ_{max} (nm)	Max. brightness (cd/m^2)	cd/A	CIE coordinates blue, white	
PF50AN50	442(544, 548)	145	0.018	(0.20, 0.22)	(0.30, 0.36)
PF75AN25	442(538)	285	0.031	(0.23, 0.28)	(0.30, 0.36)
PF90AN10	450(538)	154	0.015	(0.20, 0.23)	(0.30, 0.35)
PF	436	46.2	0.003	(0.18, 0.13)	

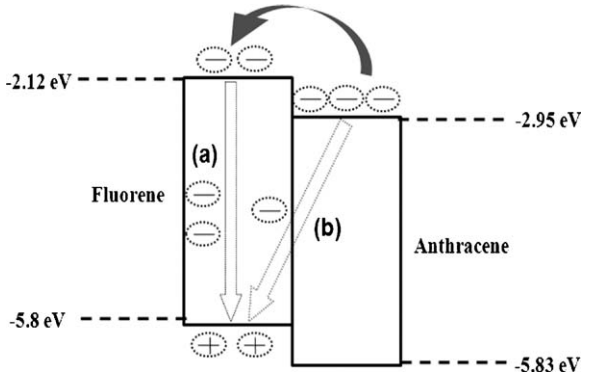

Fig. 7. Energy band diagram of (a) exciton emission (b) electroplex.

4. Conclusion

We have successfully synthesized a new polymer using the blue-emitting materials anthracene and fluorene, and this polymer demonstrates excellent solubility and thermal stability. PF50AN50, PF75AN25, and PF90AN10 demonstrate maximum photoluminescent wavelengths when λ_{max} = 440, 440, and 443 nm and peaks for electroluminescent properties when λ_{max} = 442, 442, and 450 nm, respectively. The EL emission spectra are shown to be blue-shifted compared to the PL emission spectra. It is especially noteworthy that the electroplex emission generates a new emission band. New electroplex-increased emission peaks appear nearby 540 nm at 13 V, 14 V, and 15 V, respectively, as driving voltage increases, with the CIE coordinates being (0.30, 0.36) and change in color observed from blue emission to white emission. In conclusion, we have used blue materials in a single component to observe the electroplex phenomenon.

Acknowledgement

This paper was supported by Konkuk University in 2010.

References

[1] R.H. Friend, R.W. Gymer, A.B. Holmes, J.H. Burroughes, R.N. Marks, C. Taliani, D.D.C. Bradley, D.A. Dos Santos, J.L. Bredas, M. Logdlund, W.R. Salaneck, Nature (London) 397 (1999) 121.
[2] C.W. Tang, S.A. Van Slyke, Appl. Phys. Lett. 51 (1987) 913.
[3] B. Liu, W.L. Yu, Y.H. Lai, W. Huang, Macromolecules 33 (2000) 8945.
[4] S.Y. Oh, C.H. Lee, S.H. Ryu, H.S. Oh, J. Ind. Eng. Chem. 12 (2006) 69.
[5] J.Y. Lee, Y.J. Kwon, J.W. Woo, D.K. Moon, J. Ind. Eng. Chem. 14 (2008) 810.
[6] B.L. Lee, T. Yamamoto, Macromolecules 32 (1999) 1375.
[7] I. Mcculloch, M. Heeney, C. Bailey, K. Genevicius, I. Macdonald, M. Shkunov, D. Sparrowe, S. Tierney, R. Wagner, W. Zhang, M.L. Chabinyc, R.J. Kline, M.D. Mcgehee, M.F. Toney, Nat. Mater. 5 (2006) 328.
[8] T. Yasuda, T. Imase, T. Yamamoto, Macromolecules 38 (2005) 7378.
[9] A. Tanimoto, T. Yamamoto, Macromolecules 39 (2006) 3546.
[10] S. Samitsu, Y. Takanishi, J. Yamamoto, Macromolecules 42 (2009) 4366.
[11] G. Lu, H. Usta, C. Risko, L. Wang, A. Facchetti, M.A. Ratner, T.J. Marks, J. Am. Chem. Soc. 130 (2008) 7670.
[12] J. Gao, G. Yu, A.J. Heeger, Adv. Mater. 9 (10) (1998) 692.
[13] M.D. McGehee, A.J. Heeger, Adv. Mater. 22 (12) (2000) 1655.
[14] J.Y. Lee, S.W. Heo, H.L. Choi, Y.J. Kwon, J.R. Haw, D.K. Moon, Sol. Energy Mater. Sol. Cells 93 (2009) 1932.
[15] J.Y. Lee, W.S. Shin, J.R. Haw, D.K. Moon, J. Mater. Chem. 19 (2009) 4938.
[16] B.Y. Myung, J.J. Kim, T.H. Yoon, J. Polym. Sci. Polym. Chem. 40 (2002) 4217.
[17] K. Miyatake, T. Yasuda, M. Hirai, M. Nanasawa, M. Watanabe, J. Polym. Sci. Polym. Chem. 45 (2007) 157.
[18] G. Gustafsson, Y. Cao, G.M. Treacy, F. Klavetter, N. Colaneri, A.J. Heeger, Nature 357 (1992) 477.
[19] A.J. Heeger, Solid State Commun. 107 (1998) 673.
[20] M.M. Alam, S.A. Jenekhe, Chem. Mater. 14 (2002) 4775.
[21] J.H. Burroughes, D.D. Bradley, A.R. Brown, R.N. Marks, K. Mackay, R.H. Friend, P.L. Burns, A.B. Holmes, Nature 347 (1990) 539.
[22] Q. Pei, Y. Yang, J. Am. Chem. Soc. 118 (1996) 7416.
[23] D.H. Hwang, S.K. Kim, M.J. Park, J.H. Lee, B.W. Koo, I.N. Kang, S.H. Kim, T. Zyung, Chem. Mater. 16 (2004) 1298.
[24] A. Iraqi, I. Wataru, Chem. Mater. 16 (2004) 442.
[25] Z. Tan, R. Tang, E. Zhou, Y. He, C. Yang, F. Xi, Y. Li, Appl. Polym. Sci. 107 (2008) 514.
[26] Q. Hou, Y. Xu, W. Yang, M. Yuan, J. Peng, Y. Cao, J. Mater. Chem. 12 (2002) 2887.
[27] M.J. Park, J.H. Lee, I.H. Jung, J.H. Park, D.H. Hwang, H.K. Shim, Macromolecules 41 (2008) 9643.
[28] B.W. D'Andrade, R. Forrest, Adv. Mater. 16 (2004) 1585.
[29] S.K. Lee, T. Ahn, N.S. Cho, J.I. Lee, Y.K. Jung, J. Lee, H.K. Shim, J. Polym. Sci. Polym. Chem. 45 (2007) 1199.
[30] M. Grell, X. Long, D.D.C. Bradely, M. Inbasekaran, E.P. Woo, Adv. Mater. 9 (1997) 798.
[31] N.S. Cho, D.H. Hwang, J.I. Lee, B.J. Jung, H.K. Shim, Macromolecules 35 (2002) 1224.
[32] A. Charas, J. Morgado, J.M.G. Martinho, L. Alcácer, S.F. Lim, R.H. Friend, F. Cacialli.
[33] J. Liu, Z. Xie, Y. Cheng, Y. Geng, L. Wang, X. Jing, F. Wang, Adv. Mater. 19 (2007) 531.
[34] J. Luo, X. Li, Q. Hou, J. Peng, W. Yang, Y. Cao, Adv. Mater. 19 (2007) 1113.
[35] J. Liu, Y. Cheng, Z. Xie, Y. Geng, L. Wang, X. Jing, F. Wang, Adv. Mater. 20 (2008) 1357.
[36] S. Setayesh, A.C. Grimsdale, T. Weil, V. Enkelmann, K. Müllen, F. Meghdadi, E.J.W. List, G. Leising, J. Am. Chem. Soc. 123 (2001) 946.
[37] M.R. Craig, M.M. de Kok, J.W. Hofstraat, A.P.H.J. Schenning, E.W. Meijer, J. Mater. Chem. 13 (2003) 2861.
[38] D.K. Moon, K. Osakada, T. Maruyama, Macromolecules 26 (1993) 6992.
[39] Y.H. Kim, D.C. Shin, S.H. Kim, C.H. Ko, H.S. Yu, Y.S. Chae, S.K. Kwon., Adv. Mater. 13 (2001) 1690.
[40] S. Tao, S. Xu, X. Zhang, Chem. Phys. Lett. 429 (2006) 622.
[41] J.Y. Lee, M.H. Choi, D.K. Moon, J.R. Haw, J. Ind. Eng. Chem. 16 (2010) 395.
[42] M. Mazzeo, D. Pisignnano, F.D. Sala, J. Thompson, R.I.R. Blyth, G. Gilgli, R. Cingolani, Appl. Phys. Lett. 82 (2003) 334.
[43] Y.Z. Lee, X. Chen, M.C. Chen, S.A. Chen, J.H. Hsu, W. Fann, Appl. Phys. Lett. 79 (2001) 308.
[44] J.S. Kim, B.W. Seo, H.B. Gu, Synth. Met. 132 (2003) 285.
[45] T.Q. Nguyen, I.B. Martini, J. Lei, B.J. Schwartz, J. Phys. Chem. B 104 (2000) 237.
[46] Y. Wang, S.L. Zhao, F.J. Zhang, G.C. Yuan, Z. Xu, Microelectron. J. 38 (2007) 275.
[47] Y. Wang, F. Teng, Z. Xu, Y. Hou, Y. Wang, X. Xu, Eur. Polym. J. 41 (2005) 1020.
[48] H. Cho, D.H. Hwang, J.D. Lee, N.S. Cho, S.K. Lee, J.H. Lee, Y.K. Jung, H.K. Shim, J. Polym. Sci. 46 (2008) 979.